Magnetoluminescence studies of $In_yAl_{1-y}As$ self-assembled quantum dots in $Al_xGa_{1-x}As$ matrices

P. D. Wang and J. L. Merz
Department of Electrical Engineering, University of Notre Dame, Notre Dame, Indiana 46556

S. Fafard,* R. Leon,† D. Leonard, G. Medeiros-Ribeiro, M. Oestreich, and P. M. Petroff
Center for Quantized Electronic Structures (QUEST), Materials Department, and Department of Electrical and Computer Engineering, University of California, Santa Barbara, California 93106

K. Uchida and N. Miura
Institute for Solid State Physics, University of Tokyo, Roppongi, Minato-Ku, Tokyo 106, Japan

H. Akiyama and H. Sakaki
Research Center for Advanced Science and Technology, University of Tokyo and Quantum Transition Project, Research Development Corporation of Japan, 4-6-1 Komaba, Meguro-Ku, Tokyo, Japan

(Received 15 January 1996)

We have studied the photoluminescence spectra of $In_yAl_{1-y}As$ self-assembled quantum dots in $Al_xGa_{1-x}As$ matrices with magnetic fields up to $B=40$ T. The quantum dot structure is pseudomorphically grown by molecular-beam epitaxy on (100) GaAs substrates. From the analysis of the diamagnetic shift of the magnetoluminescence spectra, we estimate the total lateral electron and hole confinement energy to be 43 meV. The exciton radius is deduced as 5 nm. The exciton binding energy in such a quantum dot system is estimated to be ~ 31 meV based on trial wave-function calculations of the actual dot system. [S0163-1829(96)07623-0]

I. INTRODUCTION

Self-assembled quantum dots[1–4] (QD's) formed in highly strained semiconductor heterostructures show very strong zero-dimensional (0D) quantum confinement effects with δ-function-like density of states.[5–7] Highly strained layer systems result in what is known as Stranski-Krastanov[8] growth, where growth starts two dimensionally, but after a certain critical thickness is reached, islands are formed spontaneously, and a thin wetting layer is left under the islands. In this process, the growth is interrupted immediately after the formation of the islands and before strain relaxation and misfit dislocations occur. Such *in situ* formation of 0D quantum dots results in high-quality defect-free materials. In addition, the coherent islanding and strain effects can produce QD's with a size uniformity within $\pm 10\%$, which is very promising for 0D quantum devices where the sharper density of states is exploited.

In a strong 3D quantum confinement regime where the characteristic radius r_0 is approaching the bulk exciton Bohr radius a_B, the strong confinement effects overcome the Coulomb effects. The resulting spectra are very similar to those obtained without excitonic effects.[9] However, the Coulomb attraction strongly enhances the oscillator strength and gives rise to a divergent Coulomb shift $\sim 1/r$ as compared to the size quantization effects $\sim 1/r^2$.[10,11] In this paper we study magnetoluminescence to investigate the relative importance of quantum confinement and Coulomb effects in self-assembled quantum dots.

II. EXPERIMENTAL RESULTS

The self-assembled dot layer is pseudomorphically grown by MBE on a (100) GaAs substrate, and the QD's are formed by the coherent relaxation into islands of a few monolayers of $In_{0.55}Al_{0.45}As$ between $Al_{0.35}Ga_{0.65}As$ buffer and cap layers. These compositions were chosen to obtain large direct band gaps for the $Al_xGa_{1-x}As$ layers, and to raise the band gap in the QD layers without undergoing the indirect transition for $In_xAl_{1-x}As$ (the direct-indirect transition corresponds to 68% Al in $In_xAl_{1-x}As$ ternary alloy). From TEM plan-view and cross-sectional measurements, the QD diameter, thickness, and density were measured. A narrow normal distribution of $2r=17.9\pm 2.1$ nm was found for the diameter with a density of $\sim 200\ \mu m^{-2}$ and a thickness to diameter ratio of ~ 0.18. A detailed account of the growth and general photoluminescence (PL) properties of these QD's has been published previously.[12,13] The magnetic fields were generated with a pulsed magnet and PL spectra at 4.2 K were detected using an optical multichannel analyzer system, where the PL spectra were obtained by use of an Ar^+ laser light with a wavelength of 514.5 nm.[14] The pulse duration of the magnetic field was 10 msec and its variation during the measurement was within $\pm 3\%$ at the top of the pulsed magnetic field. Both Faraday ($B\|Z$) and Voigt ($B\perp Z$) geometries with light propagating along the Z (growth) direction were used in the present magneto-PL measurement.

Magneto-PL spectra up to 40 T are plotted in Fig. 1. The high-energy peak at 1.994 eV is the luminescence from $Al_{0.35}Ga_{0.65}As$ buffer and barrier layers while the low-energy broad peak at 1.894 eV is from $In_{0.55}Al_{0.45}As$ QD's.[15] The broad peak with FWHH (full width at half height) of 46 meV is typical of the case where a large number of QD's were probed. It reflects the statistical distribution of ground-state energy levels of individual dots with slightly different con-

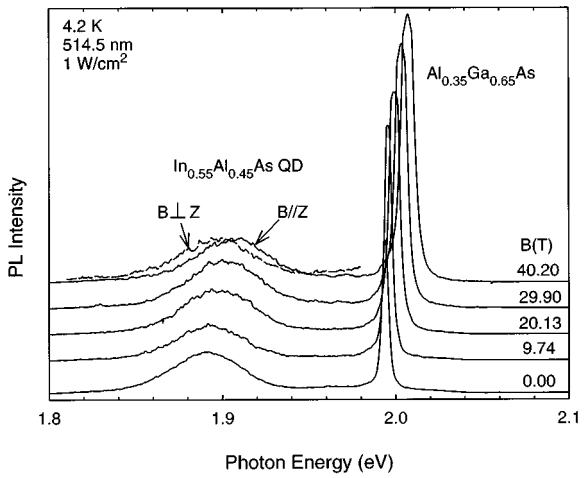

FIG. 1. Magneto-PL spectra of $In_{0.55}Al_{0.45}As$ self-assembled quantum dots under both Faraday ($B\|Z$) and Voigt ($B\perp Z$) configurations. Note that PL from bulk $Al_{0.35}Ga_{0.65}As$ material was saturated in high magnetic fields. However, the peak can still be determined accurately.

fining potentials. PL from individual quantum dots can be observed when only a small number of QD's are probed.[6] The PL peak positions for both configurations are plotted as a function of magnetic field in Fig. 2. As shown in this figure, the bulk PL peak shifts for $Al_{0.35}Ga_{0.65}As$ are almost equally independent of the two configurations in all the magnetic field regions. In the low-field region ($B<15$ T), the PL peak positions are diamagnetically shifted with the diamagnetic coefficient of 16 ± 2 $\mu eV/T^2$. With increasing magnetic field, the cyclotron energy associated with the magnetic field overcomes the Coulomb energy of electron and holes. At this point, the peak energy shifts linearly and becomes parallel to the first Landau level of electron and hole transitions.[16] From the low-field quadratic diamagnetic shift, the exciton binding energy for this 3D $Al_{0.35}Ga_{0.65}As$ material can be derived as 8.1 meV, in excellent agreement with simple effective-mass approximations.

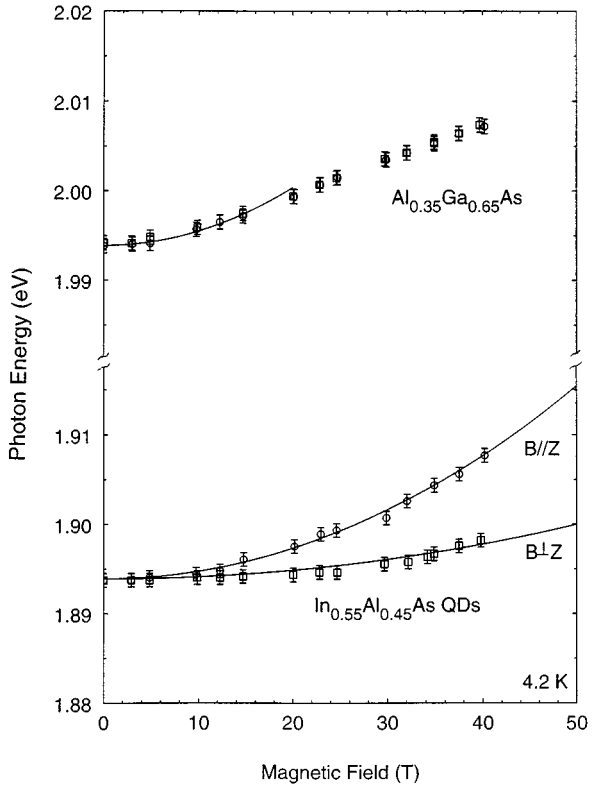

FIG. 2. Photoluminescence peak positions from QD's and bulk material as a function of magnetic field. The solid line is a parabolic curve fitting to the peak positions, from which the diamagnetic coefficients were determined.

The effective exciton confinement in quantum dots can also be revealed by studying the PL shifts of the QD's. As expected, the PL peak shifts of QD's are clearly dependent on the two field configurations, since the geometrical lengths of the QD's are very different. In both $B\|Z$ and $B\perp Z$ configurations, the PL peak shifts quadratically up to 40 T with coefficients β of 8.5 ± 0.9 and 2.6 ± 0.4 $\mu eV/T^2$, respectively, demonstrating the stronger confinement effects and Coulomb attraction between electrons and holes. In addition, it confirms the anisotropic shape of QD's along the growth and lateral directions. In QD magnetoluminescence at low fields, the magnetic field can be treated as a small perturbation. Then, the diamagnetic energy shift can be expressed as $\Delta E=\beta B^2$ with $\beta=e^2\langle\rho^2\rangle/8\mu$.[17,18] For $In_{0.55}Al_{0.45}As$ the exciton reduced mass is taken as $0.0647m_0$. Based on the experimentally determined diamagnetic shift, the average effective exciton radius $\sqrt{\langle\rho^2\rangle}$ in these QD's is estimated to be 5 nm, smaller than the QD radius of $\sim$9 nm as given above. Note that in an ideal 2D $In_{0.55}Al_{0.45}As$ QW, the in-plane exciton radius is $\sqrt{3/8}a_B=6.4$ nm with 3D exciton Bohr radius $a_B=10.4$ nm. The above analysis shows the truly 0D quantum confinement in the system, which squeezes the exciton wave function beyond its 2D limit. It should be noted that the lateral quantum confinement rather than the electron-hole correlation effect shrinks the exciton as r decreases.[10]

III. DISCUSSION

In order to interpret the experimental results in the high-magnetic-field region, where the Coulomb interaction can be approximately neglected, the following parabolic potential is employed as the in-plane confining potential:

$$V=\tfrac{1}{2}m_e^*\omega_\rho^2\rho^2.$$

Here the contribution by holes is assumed to be small and neglected because of their large effective mass ($\sim 0.4m_0$). The electron effective mass in $In_{0.55}Al_{0.45}As$ is $0.076m_0$. When the magnetic field is applied perpendicular to the QD plane, the ground-state energy shift is represented as follows:[19]

$$\Delta E=\tfrac{1}{2}\hbar\sqrt{\omega_c^2+4\omega_\rho^2},$$

where $\omega_c=eB/m_e^*$ is the electron cyclotron frequency. By fitting the above equation to the experimental data (see Fig. 2, $B\|Z$ curve of $In_{0.55}Al_{0.45}As$), the lateral confining potential is estimated as $\hbar\omega_\rho\sim43$ meV. Assuming a cylindrical quantum disk with infinite potential barrier, the electron confinement energy is $E_e=\hbar^2k_{10}^2/2m_e^*\sim37$ meV. Here $k_{10}r=2.4048$ (the first node of zero-order Bessel function).

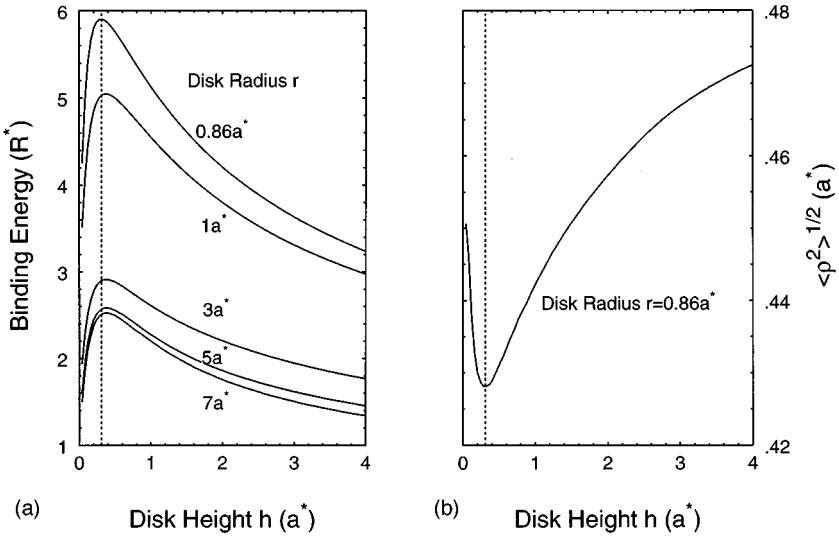

FIG. 3. (a) Normalized exciton binding energy as a function of normalized quantum disk height for different disk radii. (b) The effective exciton radius as a function of quantum disk height for its radius of $r=0.86a^*$. The normalization parameters are the 3D exciton Bohr radius a^* and ground-state effective Rydberg R^*. The vertical dotted line indicates the quantum disk height in $In_xAl_{1-x}As$ QD's.

This value is slightly smaller than $\hbar\omega_\rho$. This may be due to the hole confinement energy, which is neglected in the fitting of experimental data. In fact, in the model of infinite potential barrier, the lateral hole confinement can be calculated as $E_h \sim 4$ meV. Therefore, the total confinement energy is $E_e+E_h \sim 41$ meV, very close to the experimental value (43 meV). Other factors influencing the confinement energy include the assumption of parabolic potentials, the difference between the actual cross-section shape of self-assembled quantum dots, and the cylindrical quantum disk model employed here. Nevertheless, the cylindrical quantum disk model with infinite potential seems to give a reasonable account of confinement energies in self-assembled quantum dots.

To estimate the exciton binding energy, we adopt a variational approach[20] to calculate the ground-state energy and its eigenfunction. We consider an isolated cylindrical $In_xAl_{1-x}As$ disk of radius r and height h embedded in an infinitely larger $Al_xGa_{1-x}As$ crystal. The effective Hamiltonian reads

$$H=-\frac{\hbar^2}{2m_e^*}\nabla^2-\frac{\hbar^2}{2m_h^*}\nabla_h^2-\frac{e^2}{4\pi\epsilon_0\epsilon_r(\mathbf{r}_e-\mathbf{r}_h)}+V_e(\mathbf{r}_e)+V_h(\mathbf{r}_h).$$

$V_e(\mathbf{r}_e)$ and $V_h(\mathbf{r}_h)$ are the electron and the hole well potential arising from the band offset of QD's and cladding layers. To be more realistic with the actual QD system and to estimate accurately the exciton binding energy, we choose the following finite potential barrier:

$$V_i(\mathbf{r}_i)=V_i\Theta(\rho_i-r)\Theta(|z_i|-h/2),$$

with $i=e,h$. Here $\Theta(x)$ is the step function [$\Theta(x)=1$ if $x>0$ and $\Theta(x)=0$ if $x<0$]. z_e and z_h are the electron and hole coordinates along the cylinder axis chosen as the z axis, and ρ_e and ρ_h are the electron and hole coordinates in the plane perpendicular to the cylinder axis. For $In_{0.55}Al_{0.45}As$-$Al_{0.35}Ga_{0.65}As$ strained heterostructures, the total heavy-hole band offset is $\Delta E_g=430$ meV (the light hole has a type-II band alignment). From the model-solid theory of Van de Walle,[21] we calculate the conduction-band offset as $Q_c \sim 60\%$. The trial wave function is chosen as

$$\Psi_{eh}=\psi_e(\rho_e,z_e)\psi_h(\rho_h,z_h)\psi_{eh}(\rho_{eh},|z_e-z_h|),$$

where the product function $\psi_e\psi_h$ describes the confinement of uncorrelated electron-hole pair and ψ_{eh} describes the internal motion of the exciton. To avoid the occurrence of fourfold integrals, which leads to heavy numerical computations,[22] we choose a simplified trial function for the internal motion of the exciton:

$$\psi_{eh}(\rho_{eh},|z_e-z_h|)=\exp\left(-\frac{\rho_{eh}}{\alpha}\right)\exp\left(-\frac{|z_e-z_h|^2}{\lambda^2}\right).$$

Here α,λ are variational parameters, which are determined by minimizing the system eigenenergies $\langle E(\alpha,\lambda)\rangle$ of Hamiltonian H. To study the influence of confinement on the Coulomb interaction, we define the exciton binding energy as

$$E_B=E_e+E_h-\langle E(\alpha,\lambda)\rangle.$$

E_e and E_h are uncorrelated electron and hole confinement energies, respectively. The detailed mathematical formula has been shown in Ref. 20. Here the numerical results are presented. Figure 3(a) shows the exciton binding energy as a function of disk height h for different disk radius r. Here we choose the effective exciton Bohr radius $a^*=4\pi\epsilon_0\epsilon_r\hbar^2/\mu e^2=104$ Å of the 3D $In_{0.55}Al_{0.45}As$ exciton for the unit of length and the effective ground-state Rydberg $R^*=e^2/8\pi\epsilon_0\epsilon_r a^*=5.45$ meV for the unit of energy. In $In_{0.55}Al_{0.45}As$ QD's studied here, the disk height and radius are $0.31a^*$ and $0.86a^*$, respectively. It should be noted that the trial function proposed here reproduces the 2D case very well for large disk radius ($r>7a^*$) where the lateral confinement is negligible. For the $In_{0.55}Al_{0.45}As$ dots studied here, the quantum disk height should be $0.31a^*$ with a disk radius of $0.86a^*$. The exciton binding energy is estimated as $5.8R^* \approx 31$ meV. The effective exciton radius $\sqrt{\langle\rho^2\rangle}$ is plotted in Fig. 3(b) for a $r=0.86a^*$ QD by using the same trial function. For our $In_{0.55}Al_{0.45}As$ quantum dots, the effective exciton radius $\sqrt{\langle\rho^2\rangle} \approx 0.43a^*=4.4$ nm is close to the value (5 nm) derived from experimental diamagnetic shift. There-

fore, our results should closely reproduce the experimental diamagnetic shift in Fig. 2 based on a first-order perturbation theory.

Our simplified model agrees reasonably well with more sophisticated calculations assuming different confining potential[23] or different shape of the quantum disk.[10] For example, from Fig. 5 of Ref. 10 the ratio of exciton binding energy to the confinement energy should be ~ 0.7 for a 20-nm^2 disk. This value is close to our results of $E_B/(E_e+E_h)=0.72$.

IV. CONCLUSION

We have studied the magneto-PL spectra of $In_{0.55}Al_{0.45}As$ self-assembled quantum dots and derived many fundamental excitonic parameters. The results demonstrate clearly the 3D quantum confinement effects with enhanced exciton binding energy. The superior structural quality (narrow size distributions and defect-free materials) and enhanced optical properties (high exciton binding and strong quantum confinement) promise a new generation of 0D low-threshold semiconductor lasers and other optoelectronic devices.

ACKNOWLEDGMENTS

Support from QUEST, an NSF Science and Technology Center for Quantized Electronic Structures (Grant No. DMR 91-20007), and the NSF International Program (Grant No. INT 93-21727) are gratefully acknowledged.

*Present address: Institute of Microstructural Science, National Research Council, Ottawa, Canada K1A 0R6.

†Present address: Department of Electronic Materials Engineering, The Australian National University, Canberra, ACT 0200, Australia.

[1] D. Leonard, M. Krishnamurthy, S. Fafard, J.L. Merz, and P.M. Petroff, J. Vac. Sci. Technol. B **12**, 1063 (1994).

[2] J.M. Moison, F. Houzay, F. Barthe, L. Leprince, E. Andre, and O. Vatel, Appl. Phys. Lett. **64**, 196 (1994).

[3] See, for, example, D. Leonard, K. Pond, and P. M. Petroff, Phys. Rev. B **50**, 11 687 (1994).

[4] R. Notzel, J. Temmyo, H. Kamada, T. Furuta, and T. Tamamura, Appl. Phys. Lett. **65**, 457 (1994).

[5] J.M. Marzin, J.M. Gerard, A. Izrael, D. Barrier, and G. Bastard, Phys. Rev. Lett. **73**, 716 (1994).

[6] S. Fafard, R. Leon, D. Leonard, J.L. Merz, and P.M. Petroff, Phys. Rev. B **50**, 8086 (1994).

[7] M. Grundmann, J. Christen, N.N. Ledentsov, J. Bohrer, D. Bimberg, S.S. Ruvimov, P. Werner, U. Richter, U. Gosele, J. Heydenreich, V.M. Ustinov, A.Yu. Egorov, A.E. Zhukov, P.S. Kop'ev, and Zh.I. Alferov, Phys. Rev. Lett. **74**, 4043 (1995).

[8] I.N. Stranski and Von L. Krastanow, Akad. Wiss. Lit. Mainz Math. Naturwiss. K1. IIb **146**, 797 (1939).

[9] B. Adolph, S. Glutsch, and F. Bechstedt, Phys. Rev. B **48**, 15 077 (1993).

[10] G.W. Bryant, Phys. Rev. B **37**, 8763 (1988).

[11] S. Jaziri and R. Bennaceur, Semicond. Sci. Technol. **9**, 1775 (1994).

[12] R. Leon, S. Fafard, D. Leonard, J.L. Merz, and P.M. Petroff, Appl. Phys. Lett. **67**, 521 (1995); Science **267**, 1966 (1995).

[13] S. Fafard, R. Leon, D. Leonard, J.L. Merz, and P.M. Petroff, Phys. Rev. B **52**, 5752 (1995).

[14] S. Tarucha, H. Okamoto. Y. Iwasa, and N. Miura, Solid State Commun. **52**, 815 (1984).

[15] The luminescence from the wetting layer was not observed in this sample under normal excitation conditions. This reflects the efficient exciton migration from the wetting layer to the QD's, which have a lower potential. In the following analysis, we neglect the contribution of the wetting layer on electron-hole confinement and Coulomb effects in $In_xAl_{1-x}As$ QD's.

[16] O. Akimoto and H. Hasegawa, J. Phys. Soc. Jpn. **22**, 181 (1967).

[17] P.D. Wang, N.N. Ledentsov, C.M. Sotomayor Torres, I.N. Yassievich, A. Pakhomov, A. Yu. Egovov, P.S. Kopev, and V.M. Ustinov, Phys. Rev. B **50**, 1604 (1994).

[18] By using the same equation, the effective exciton diameter is defined by T. Someya, H. Akiyama, and H. Sakaki, Phys. Rev. Lett. **74**, 3664 (1995). Here we employ a cylindrical coordinate system with vector potential $\mathbf{A}=\frac{1}{2}\mathbf{B}\times\mathbf{r}$ with $\mathbf{B}=B\hat{z}$; in cylindrical coordinates the magnetic field potential becomes $A_\rho=A_z=0$, $A_\phi=B\rho/2$.

[19] V. Fock, Z. Phys. **47**, 446 (1928).

[20] S. Le Goff and B. Stebe, Solid State Commun. **83**, 555 (1992).

[21] C. Van de Walle, Phys. Rev. B **39**, 1871 (1989), and references therein.

[22] Y. Kayanuma, Phys. Rev. B **44**, 13 085 (1991).

[23] V. Halonen, T. Chakraborty, and P. Pietilainen, Phys. Rev. B **45**, 5980 (1992).